Merocyanine Aggregation in Mesoporous Networks

F. Nüesch,*,† J. E. Moser, V. Shklover,‡ and M. Grätzel

Contribution from the Institut de Chimie Physique, Ecole Polytechnique Fédérale, CH-1015 Lausanne, Switzerland

Received September 5, 1995[⊗]

Abstract: Nanocrystalline films of TiO_2, Al_2O_3, and ZrO_2 were used as hosts for the merocyanine 3-acetyl-5-(2-(3-ethyl-2-benzothiazolidinylidene)ethylidene)rhodanine (Mc2) to scrutinize templating effects in the accommodation of the dye within their porous network. Composed of interconnected mesoscopic oxide particles and pores, these films are transparent, allowing for a straightforward application of transmission spectroscopy to unravel the optical features of the incorporated dye species. Apart from H-aggregation, the formation of two different types of two-dimensional assemblies was witnessed yielding red-shifted absorption bands which were identified as J-aggregates, one showing Davidov splitting, the other having a single exciton band. The herringbone packing of the dye molecules in the layered structure of Mc2 sodium salt octahydrate single crystals was taken to model the double-banded J-aggregate structure. On mesoscopic hydroxylated TiO_2 anatase films, the structure of the Mc2 assemblies is controlled by the texture of the highly porous substrates as well as their surface charge. Furthermore, it responds in a striking fashion to the presence of solvent in the ambient to which the films are exposed. Double-banded (herringbone structure) and single-banded (parallel alignment of the dye) absorption spectra can thus be obtained. The role of solvent is to stabilize one particular aggregate geometry through intercalation into the Mc2 aggregate. Electron injection into TiO_2 from both types of J-aggregates is observed. Laser flash photolysis experiments show that energy transfer from the monomer to the J-aggregate is operative prior to charge injection. On hydroxylated Al_2O_3 and ZrO_2 surfaces Mc2 undergoes physisorption and formation of H-aggregates exhibiting a blue-shifted absorption with regard to the monomer spectrum. Contrary to the results obtained for TiO_2 substrates, aggregation is hardly influenced by solvent in the ambient. In particular no J-aggregates can be formed on bare Al_2O_3 and ZrO_2 substrates. However, when the porous films are impregnated with concentrated hydroxide solutions, H- as well as J-aggregates are formed in humid air. At high humidity, due to the hygroscopic salt coating, the pores are completely filled with water, leading to the precipitation of the dye molecules forming H-aggregates. At lower humidity an air−water interface builds up within the pores and a double-banded J-aggregate spectrum appears. The spectrum is almost identical to the one measured on Mc2 sodium salt octahydrate single crystals with a layered organic−inorganic structure. Resonance fluorescence originating from the energetically lower exciton band and internal conversion from the higher to the lower exciton band take place.

Introduction

The self-assembly of organic dyes to form aggregates of different size and morphology ranging from simple dimers to three-dimensional microcrystals is currently the focus of widespread attention in fundamental and applied research. J-aggregates (named after one of its discoverers) were discovered by E. E. Jelly[1] and G. Scheibe[2] in the late 1930s and have been of particular interest. The unique long-range molecular stacking order present in this type of aggregate produces an intense, narrow absorption peak which is red shifted with respect to that of the monomeric dye. Typically the fluorescence of these aggregates occurs at almost the same wavelength as the absorption, which is known as resonance fluorescence. Numerous dyes have been found to form J-aggregates, among which the cyanines,[1,3−8] merocyanines,[9−11] and squaraines[12−15] are the best represented classes.

Cyanines are a very important class of dye molecules due to their use as spectral sensitizers in the photographic process.[4,5,7,16−23] The molecular orientation and structure of

† Present address: Laboratoire de physique des solides semi-cristallins, Département de Physique, Ecole Polytechnique Fédérale, CH-1015 Lausanne, Switzerland.

‡ Present address: Laboratorium für Kristallographie, Eidgenössische Technische Hochschule, CH-8092 Zürich, Switzerland.

⊗ Abstract published in *Advance ACS Abstracts,* May 1, 1996.

(1) Jelly, E. E. *Nature* **1936**, *138*, 1009.
(2) Scheibe, G. *Angew. Chem.* **1937**, *50*, 51.
(3) Scheibe, G. *Kolloid-Z.* **1938**, *82*, 1.
(4) Herz, A. H.; Danner, R. P.; Janasonis, G. A. In *Adsorption from Aqueous Solution*; American Chemical Society: Washington, DC, 1967; Vol. 79, p 173.
(5) Steiger, R.; Kitzing, R.; Junod, P. *J. Photogr. Sci.* **1973**, *21*, 107.
(6) Smith, D. L. *Photogr. Sci. Eng.* **1974**, *18*, 309.
(7) Maskasky, J. E. *Langmuir* **1991**, *7*, 407.
(8) Kirstein, S.; Möhwald, H. *Chem. Phys. Lett.* **1992**, *189*, 408.
(9) Inoue, T. *Thin Solid Films* **1985**, *132*, 21.
(10) Nakahara, H.; Fukuda, K.; Möbius, D.; Kuhn, H. *J. Phys. Chem.* **1986**, *90*, 6144.
(11) Wolthaus, L.; Schaper, A.; Möbius, D. *Chem. Phys. Lett.* **1994**, *225*, 322.
(12) Morel, D. L.; Ghosh, A. K.; Feng, T.; Stogryn, E. L.; Purwin, P. E.; Shaw, R. F. *Appl. Phys. Lett.* **1978**, *32*, 495.
(13) Kim, S.; Furuki, M.; Pu, L. S.; Nakahara, H.; Fukuda, K. *Thin Solid Films* **1988**, *159*, 337.
(14) Liang, K.; Law, K. Y.; Whitten, D. G. *J. Am. Chem. Soc.* **1994**, *98*, 13379.
(15) Kim, Y.-S.; Liang, K.; Law, K.-Y.; Whitten, D. G. *J. Phys. Chem.* **1994**, *98*, 984.
(16) James, T. H. *The theory of the photographic process*; Macmillan: New York, 1977.
(17) Herz, A. H. *Adv. Colloid Interface Sci.* **1977**, *8*, 237.
(18) Muenter, A. A.; Brumbaugh, D. V.; Apolito, J.; Horn, L. A.; Spano, F. C.; Mukamel, S. *J. Phys. Chem.* **1992**, *96*, 2783.
(19) Tani, T.; Suzumoto, T.; Kemnitz, K.; Yoshihara, K. *J. Phys. Chem.* **1992**, *96*, 2778.
(20) Tani, T.; Kikuchi, S.-I. *Bull. Soc. Sci. Photogr. Jpn.* **1967**, *17*, 1.
(21) Bird, G. R.; Norland, K. S.; Rosenoff, A. E.; Michaud, H. B. *Photogr. Sci. Eng.* **1968**, *12*, 196.
(22) Gilman, Jr., P. B. *Photogr. Sci. Eng.* **1974**, *18*, 418.
(23) Scrutton, S. L. *J. Photogr. Sci.* **1974**, *22*, 69.
(24) Steiger, R.; Kitzing, R.; Hagen, R.; Stoeckli-Evans, H. *J. Photogr. Sci.* **1974**, *22*, 151.

S0002-7863(95)03042-3 CCC: $12.00

cyanine J-aggregates adsorbed on silver halides have indirectly been obtained from X-ray single-crystal structures,[6,24−26] theoretical calculations of aggregate wavelength shifts relative to molecular orientations,[27−30] polarization absorption and fluorescence measurements,[7,8] and the SEM technique.[31] The role of aggregation on the sensitizing properties of the dye has been of great interest in the photographic industry.[32,33] Self-supersensitization by J-aggregates involving electron transfer from the monomer to the J-aggregate has been reported.[34] In other systems cyanine J-aggregates have been shown to inhibit sensitization.[35] The exciton dynamics in J-aggregates were first investigated on monolayers of an oxacyanine dye.[36] Recently experimental data on the exciton dynamics of pseudoisocyanine in solution[37,38] and on silver halides[18] has been discussed in the framework of exciton theory.

Instead of two nitrogens for cyanines, merocyanine dyes are characterized by a polymethine chain connecting a nitrogen and an oxygen atom. They have also proven to be efficient sensitizers.[16,39,40] The striking photoconductive properties of evaporated merocyanine dye layers have attracted much attention in the field of solar energy conversion.[12,41−45] The best candidates for organic solar cells have been derivatives of 3-acetyl-5-(2-(3-ethyl-2-benzothiazolidinylidene)ethylidene)-rhodanine (Mc2), which is the dye studied in this work.

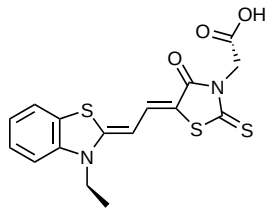

Mc2

Intensive work on J-aggregate films produced by the Langmuir−Blodgett technique has yielded information about interplanar distance and slipping angles for J-aggregates of octadecyl-substituted Mc2 merocyanines.[10,46,47] The orientation of the dye at the air−subphase interface has been controlled via hydrophobic alkyl chains that are also proposed to stabilize the two-dimensional aggregate structure. Absorption and emission spectroscopy have provided useful information on the adsorption geometry. Recently the molecular packing of another amphiphilic merocyanine dye has been determined by the AFM technique showing the brick stone arrangement.[11] Merocyanine J-aggregates are attracting considerable attention in various theoretical fields, too. Free radicals in merocyanine J-aggregate LB films have been detected by electron spin resonance.[48,49] The presence and absence of an inversion center for J-aggregates formed by the LB technique has been investigated and the second harmonic generation on such films discussed.[47,50] Weak exciton−phonon coupling in long-chain merocyanine J-aggregates on a LB film has also been reported.[51]

Our previous work has analyzed the columnar stacking of Mc2 molecules yielding blue-shifted absorption spectra (H-aggregates) on a metal oxide support, in small Mc2 microcrystals as well as in Mc2 single crystals.[52] This work reports for the first time J-aggregate formation of a merocyanine dye having no long alkyl substituents. Mesoscopic metal oxide particles 14−30 nm in diameter are used as substrates. These highly porous films are transparent, which allows a straightforward optical characterization. We show that aggregate structure is induced not only by physisorption and intermolecular van der Waals forces but also by the intercalation of solvent molecules. The surface morphology of the substrate is analyzed by high-resolution electron microscopy, and its influence will be discussed. Furthermore, we demonstrate a new method to form H- and J-aggregates using salt-impregnated porous substrates. Optical properties of the J-aggregates will be linked to the Mc2 sodium salt octahydrate crystal structure.[53] The layered architecture consisting of water-coordinated Na^+ planes alternating with two-dimensional dye planes is most appropriate to model the structure of two-dimensional J-aggregates. Such organic−inorganic layered crystals with J-aggregate packing of the organic molecules have never been observed before and provide the first direct measurement of a merocyanine J-aggregate geometry.

Experimental Section

Materials. Mc2 merocyanine acid was supplied by Riedl de Haën. Further purification involved recrystallization from dilute aqueous HCl.

Al_2O_3 (Alu C, Degussa) and ZrO_2 (VP, Degussa) powders constituted of 14 and 30 nm diameter particles, respectively, were spread on a glass slide before sintering.[52,54] The following procedure was used: 1 g of oxide powder was ground in an agate mortar by dropwise addition of distilled water. Aliquots of 20 μL of water were subsequently added until a viscous mass was obtained. Then 40 μL of aqueous 1 M HCl was added followed by manual grinding for about 15 min. Thereafter the white dispersion was diluted with 4 mL of water and 250 mg of Carbowax polymer (molecular weight: 20000, Fluka) was added and dissolved by stirring for several hours. Finally 40 μL of Triton X100 surfactant (BDH Chemicals) was added. The colloidal suspension was then spread on a glass slide and dried. Heating at 350 °C for 20 min in an air flow eliminated the organic content and ensured partial sintering of the particles. The porous nanocrystalline films produced

(25) Smith, D. L. *Photogr. Sci. Eng.* **1972**, *16*, 329.
(26) Potenza, J. P.; Mastropaolo, D. *Acta Crystallogr.* **1974**, *B30*, 2345.
(27) Czikklely, V.; Forsterling, H. D.; Kuhn, H. *Chem. Phys. Lett.* **1970**, *6*, 207.
(28) Davidov, A. S. *Theory of Molecular Excitons*; McGraw-Hill: New York, 1962.
(29) Dietz, F.; Kaiser, M. *J. Signalaufzeichnungsmater.* **1982**, *10*, 321.
(30) Kasha, M.; Rawls, H. R.; El-Bayoumi, M. A. *Pure Appl. Chem.* **1965**, *11*, 371.
(31) Saijo, H.; Shiojiri, M. *Phys. Status Solidi A* **1995**, *148*, K85.
(32) West, W.; Gilman, P. B., Jr. *Photogr. Sci. Eng.* **1969**, *13*, 221.
(33) Gilman, P. B., Jr.; Koszelak, T. D. *J. Photogr. Sci.* **1973**, *21*, 53.
(34) Sviridov, D. V.; Shapiro, B. I.; Kulak, A. I. *J. Photochem. Photobiol. A: Chem.* **1992**, *67*, 377.
(35) Noukakis, D.; Van der Auweraer, M.; De Schryver, F. C. *J. Phys. Chem.* **1994**, *98*, 11745.
(36) Möbius, D.; Kuhn, H. *J. Appl. Phys.* **1988**, *64*, 5138.
(37) Spano, F. C.; Kuklinski, J. R.; Mukamel, S. *J. Chem. Phys.* **1991**, *94*, 1534.
(38) Fidder, H.; Terpstra, J.; Wiersma, D. A. *J. Chem. Phys.* **1991**, *94*, 6895.
(39) Tani, T.; Kikuchi, S.-I. *Bull. Soc. Sci. Photogr. Jpn.* **1968**, *18*, 1.
(40) Leubner, I. H. *Photogr. Sci. Eng.* **1980**, *24*, 138.
(41) Ghosh, K.; Feng, T. *J. Appl. Phys.* **1978**, *49*, 5982.
(42) Meier, H.; Albrecht, W.; Tschirwitz, U.; Zimmerhackl, E.; Geheeb, N. *Ber. Bunsen-Ges. Phys. Chem.* **1977**, *81*, 592.
(43) Meier, H.; Albrecht, W. *Ber. Bunsen-Ges. Phys. Chem.* **1965**, *69*, 160.
(44) Piechowski, A. P.; Bird, G. R.; Morel, D. L.; Stogryn, E. L. *J. Phys. Chem.* **1984**, *88*, 934.
(45) Saito, K.; Yokoyama, H. *Thin Solid Films* **1994**, *234*, 526.
(46) Kawaguchi, T.; Iwata, K. *Thin Solid Films* **1990**, *191*, 173.
(47) Kajikawa, K.; Anzai, T.; Takezoe, H.; Fukuda, A. *Thin Solid Films* **1994**, *243*, 587.
(48) Kuroda, S.; Ikegami, K,.; Tabe, Y.; Saito, K.; Saito, M.; Sugi, M. *Phys. Rev. B* **1991**, *43*, 2531.
(49) Tani, T.; Sano, Y. *J. Appl. Phys.* **1991**, *69*, 4391.
(50) Kajikawa, K.; Takezoe, H.; Fukuda, A. *Jpn. J. Appl. Phys.* **1991**, *30*, L1525.
(51) Nakahara, H.; Uchimi, H.; Fukuda, K.; Tamai, N.; Yamazaki, I. *Thin Solid Films* **1989**, *178*, 549.
(52) Nüesch, F.; Grätzel, M. *Chem. Phys.* **1995**, *193*, 1.
(53) Nüesch, F.; Grätzel, M.; Nesper, R.; Shklover, V. *Acta Crystallogr.* **1996**, *B52*, 277.
(54) Kay, A. Thesis No. 1214, Ecole Polytechnique Fédérale de Lausanne, 1994.
(55) O'Regan, B.; Grätzel, M. *Nature* **1991**, *335*, 737.

by this method have a thickness of about 2 μm and are transparent, though some scattering originating from aggregated metal oxide particles cannot be avoided. Transparent colloidal films of TiO_2 were prepared according to a previously published procedure.[55] Figure 1 shows high-resolution transmission electron microscopy (HRTEM) micrographs of the sintered mesoscopic particles that were scratched off the film.

LiOH, NaOH, and KOH (Fluka, puriss.) and RbOH (Aldrich 99%, 50% wt solution in water) were used without further purification. 18-Crown-6 ether (Fluka, experimental) was used to bind the K^+ and Na^+ cations.

Mc2 was adsorbed on the colloidal films from a saturated ethanol solution or from an ethanol−toluene (1:10 v/v) mixture by dipping for 15 min. The solvents were Fluka puriss. grade.

Methods. Absorption measurements were carried out on a HP 8452A diode array spectrophotometer. Diffuse reflectance measurements were carried out on a Varian CARY 05 double-grating spectrophotometer equipped with an integrating sphere. The fluorescence spectra were obtained using a SPEX Fluorolog 112 spectrofluorimeter. For temperature control, the colloidal films were fixed on a sample holder and mounted in an Oxford Instruments DN1704 nitrogen bath cryostat equipped with an ITC-4 controller. The same cryostat was used for the laser flash photolysis experiments.

Nd:YAG laser pulses (10 ns, 530 nm) were used as the excitation source for Mc2 in conjunction with time-resolved absorption spectroscopy. Pulses from a dye laser (10 ns, 614 nm) pumped by a frequency-doubled ruby laser were used to excite in the red spectral domain.

The HRTEM study of the films was performed at 300 kV on a Philips CM 30 ST transmission electron microscope equipped with a detector for energy dispersive X-ray spectrometry and a STEM attachment. A thin single-crystal gold film was used as the internal standard for the determination of interplanar distances.

Results

Solution Properties of Mc2. Mc2 is soluble in a variety of solvents ranging from nonpolar ones like THF and dioxane to very polar liquids like ethylene glycol and water. It is soluble in linear alcohols up to pentanol, but it is too polar to be dissolved in benzene, toluene, or even dichloromethane. In water the solubility is mainly determined by the carboxylic group of the dye. A pK_a of 7.5 was determined by titration, above which the dye is well soluble. In this work we will mainly use water and aqueous salt solutions in conjunction with dye aggregation. It is therefore helpful to review some spectral properties of Mc2 in water. At concentrations of 10^{-7} M only the monomeric form is present, having absorption and fluorescence maxima at 540 and 554 nm, respectively. The extinction coefficient ϵ of Mc2 is high. For example, in water, $\epsilon_{max} = 125\,000$ 1 mol^{-1} cm^{-1}. This property is important when studying aggregation effects by optical spectroscopy, since the shift between the absorption maximum of the monomer and the aggregate is roughly proportional to ϵ. When the dye concentration is raised above 10^{-5} M in water, a new nonfluorescent band at 502 nm appears that has been attributed to the dimer of Mc2.[52] H-aggregation can also be induced at the surface of colloidal metal oxide particles suspended in water. The columnar stacking of dye molecules has been shown to yield blue-shifted absorption maxima ranging from 500 to 470 nm, depending on the aggregate dimensions. Here we will discuss the aggregation phenomena of dye-loaded porous metal oxide films.

Aggregation of Mc2 Loaded on Hydroxylated Mesoscopic Metal Oxide Films. (a) Substrate Treatment. In order to ensure a hydroxylated surface, the sintered metal oxide films are boiled in distilled water for 1 h. After that, the films are protonated by soaking for 12 h in a HCl solution at pH 2.5. They are subsequently rinsed under distilled water and dried in an air flow before being dipped into a dye-saturated ethanol−

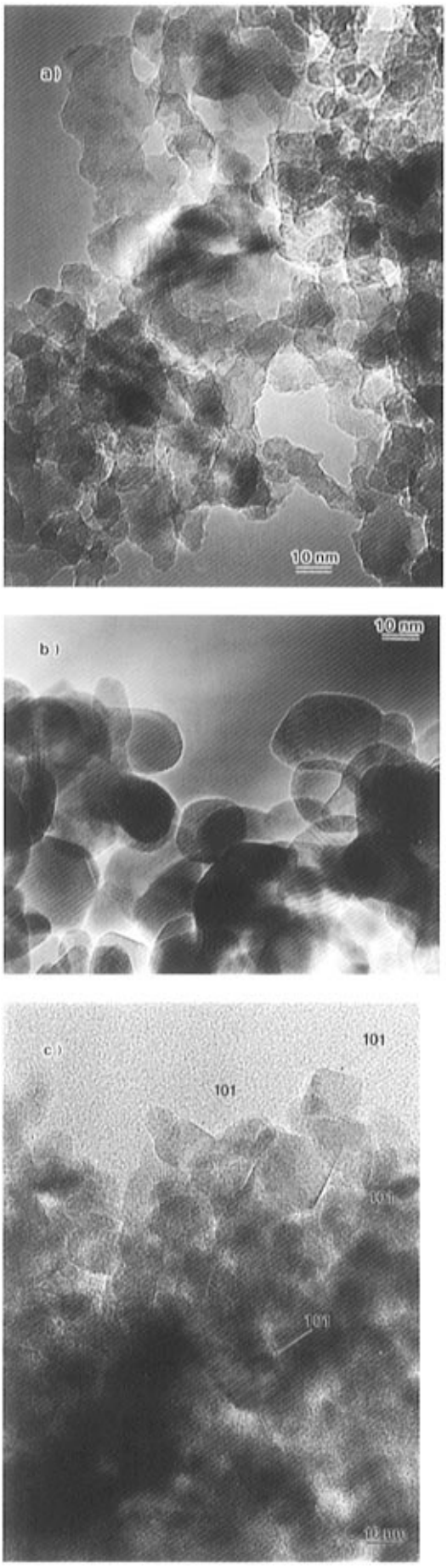

Figure 1. HRTEM micrographs of sintered metal oxide particles that were scratched off the mesoscopic films: (a) Al_2O_3; (b) ZrO_2; (c) TiO_2.

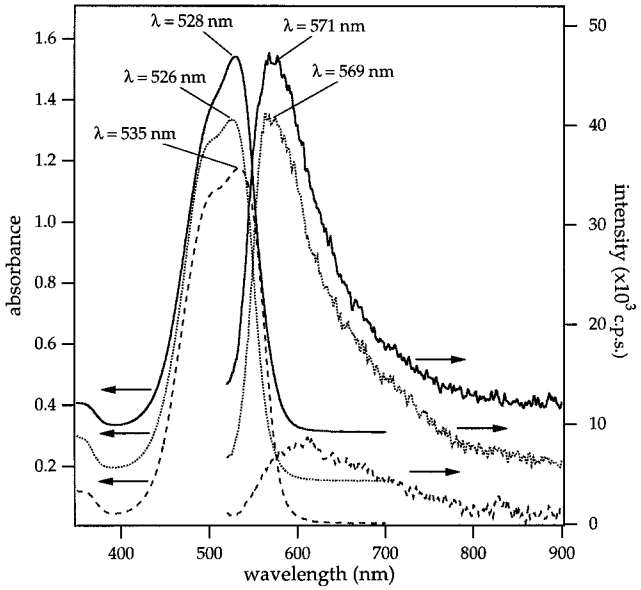

Figure 2. Absorption and fluorescence spectra of Mc2 adsorbed on Al_2O_3 under different atmospheric conditions: (—) dry atmosphere; (···) ethanol vapor; (– – –) water vapor.

toluene mixture. Subsequently, the dye-loaded substrates are brought into contact with either a solvent or solvent vapor. In the latter case we use an optical quartz cell which is flushed for 30 min with nitrogen saturated by the vapor over an alcoholic or aqueous solution. In order to analyze the substrate surface morphology the sintered particles were scratched off the glass and the powders analyzed by HRTEM. In all three cases interconnected nanoscopic particles can be distinguished (Figure 1). Furthermore, a marked difference between the three oxide particles is apparent. ZrO_2 particles are round, spherical particles with very few large surface planes. Somewhat smaller, the Al_2O_3 particles are of a highly irregular shape, showing kinks and steps. In the case of TiO_2, however, a rhombohedral shape is visible, preferentially exposing 101 surface planes.

(b) Al_2O_3 and ZrO_2 Films. The Mc2-loaded films show similar characteristics for both substrates. When the film is immersed in a dry atmosphere, the monomer absorption band dominates. The absorption maximum on Al_2O_3 at 528 nm (Figure 2) differs from the one on ZrO_2 at 537 nm due to specific interaction with the substrate. The absorption bands are broader than the solution spectrum, due to a wide distribution of different configurations of the adsorbed dye. Related to this is the relatively large Stokes shift between the absorption and fluorescence maxima. In ethanol vapor, the shoulder on the blue side of the spectrum intensifies, which indicates the formation of H-aggregates. The fluorescence yield remains quite high. The solvatochromic effect of water produces a red shift of the absorption maximum when the film is brought into contact with water vapor. Concomitantly the fluorescence yield decreases due to dimer formation. A similar spectrum is obtained when the films are immersed in acidic water.

(c) TiO_2 Films. When the dye-coated hydroxylated TiO_2 film is immersed in water at pH 2.5, a mixture of adsorbed monomers and H- and J-aggregates is observed. At pH 5−6 the equilibrium between the different conformations of adsorbed species is strongly shifted toward the H-aggregate geometry (Figure 3). Apparently this geometrical and spectral change is induced by the change from positive to negative surface charge since the 0 ζ potential of anatase particles varies from pH 5 to pH 6, depending on the preparation conditions.[56]

(56) Moser, J.; Swarnalatha, P.; Infelta, P. P.; Grätzel, M. *Langmuir* **1991**, *7*, 3012.

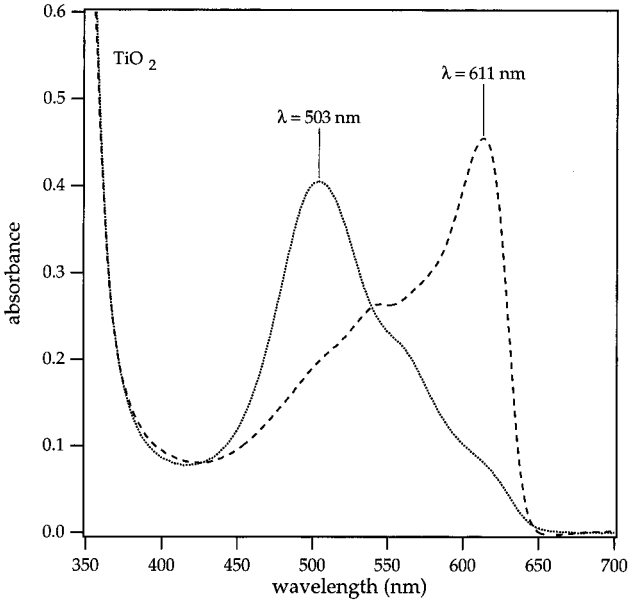

Figure 3. Absorption spectra of Mc2 adsorbed on a transparent mesoscopic TiO_2 film: (– – –) in water at pH = 2.5; (···) in water at pH = 6.

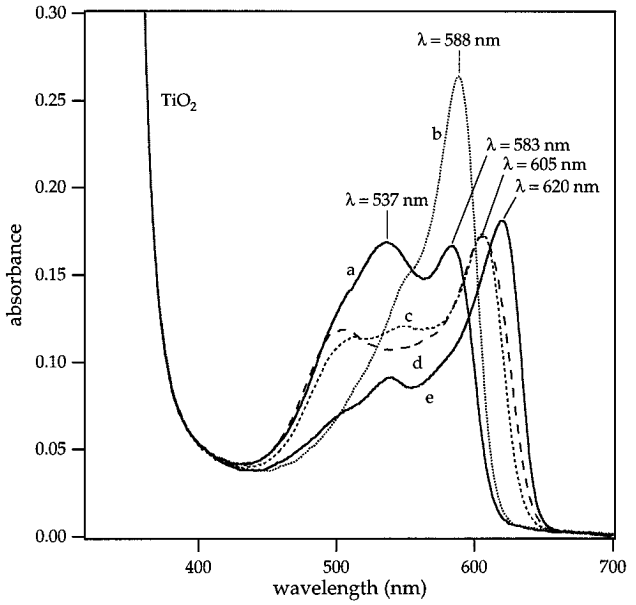

Figure 4. Absorption spectrum of Mc2 adsorbed on a transparent mesoscopic TiO_2 film in contact with the vapor of an ethanol−water mixture: (a) 1:0 (v/v); (b) 10:1 (v/v); (c) 1:1 (v/v); (d) 1:10 (v/v); (e) 0:1 (v/v).

The type of aggregation can be controlled much better when the dye-coated film is in equilibrium with solvent vapor. In pure ethanol vapor at room temperature, two absorption bands are apparent. By addition of water to the ethanol vapor a quite narrow, single red-shifted absorption band appears. A single band is also obtained under pure water vapor conditions where the 0.3 eV shift between the absorption maxima of monomeric and aggregated dye is much more important. In the vapor of an ethanol−water mixture between 10:1 and 1:10 v/v, however, a mixture of H- and J-aggregates prevails (Figure 4). Similar observations can be made using methanol and methanol−water mixtures. Under completely dry atmospheric conditions another type of adsorption showing essentially a slightly red shifted peak at 544 nm broadened by two shoulders on the blue and red sides of the absorption band appears. The shoulders correspond to H- and J-aggregates, respectively. As the humidity is increased,

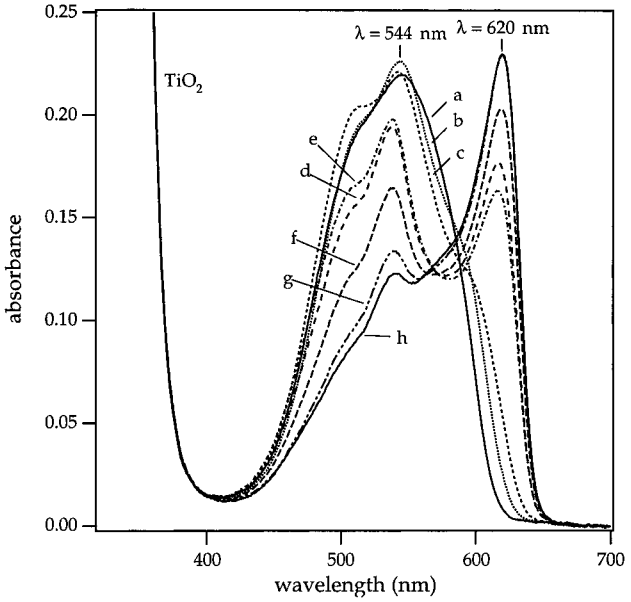

Figure 5. Absorption spectrum of Mc2 adsorbed on a mesoscopic TiO_2 film in contact with the water vapor over saturated salt solutions yielding different relative humidities (RH in %) at room temperature:[57] (a) dry; (b) NaOH (6%); (c) $CaCl_2$ (29%); (d) $Ca(NO_3)_2$ (51%); (e) KI (69%); (f) KBr (81%); (g) $BaCl_2$ (90%); (h) pure water (100%).

the broad spectral feature obtained under dry conditions gets structured clearly showing H- and J-bands. In order to control the relative humidity, the sample compartment of the quartz cell was brought into contact with the water vapor equilibrated over different saturated salt solutions (Figure 5). At about 50% humidity a double-banded absorption with maxima at 540 and 620 nm manifests, which is subsequently transformed into a spectrum showing a single absorption maximum upon raising the relative humidity.

Fluorescence of the adsorbed dye on TiO_2 is strongly quenched by charge injection into the metal oxide semiconductor. Both the signature of the absorption band located at 540 nm and that of the J-aggregate at 620 nm can be seen in the fluorescence spectrum when the excitation wavelength is 490 nm (Figure 6). J-aggregate fluorescence is observed even though the latter is not absorbing at the excitation wavelength showing energy transfer from the 540 nm absorption band to J-aggregates. No resonance fluorescence is observed. The emission maximum of the J-aggregate appears at 633 nm, slightly depending on dye loading, which gives a Stokes shift between absorption and emission maxima of roughly 0.04 eV. The location of absorption and fluorescence maxima of the absorption feature at 540 nm coincides with the respective maxima of monomeric Mc2 in water, suggesting that an equilibrium between monomers and J-aggregates is present in humid air. At low temperature the emission feature of the J-aggregate becomes quite important. It is, however, difficult to control the aggregate type when cooling down to liquid nitrogen temperatures. Water condensation at the cell walls changes the humidity, and usually a broad spectrum is obtained.

When dye loading is important and when the film is left for 2 days in humid air, a slightly different absorption and emission feature are obtained. The spectrum shows two red-shifted bands, one at 548 nm and the other at 610 nm (Figure 6). The emission spectrum, however, shows only the fluorescence from the 610 nm band, even though excitation occurs at 490 nm.

(d) Sensitization of TiO_2. Laser flash photolysis experiments demonstrate efficient electron injection into the TiO_2 conduction band according to eq 1.

$$Mc2 \xrightarrow{h\nu} Mc2^* \xrightarrow{k_{inj}} Mc2^+ + e_{cb}^-(TiO_2) \quad (1)$$

$$Mc2^+ + e_{cb}^-(TiO_2) \xrightarrow{k_b} Mc2 \quad (2)$$

When the dye is present in the form of monomers or H-aggregates, the transient spectrum shows the corresponding bleaching of these two species. In both cases a new species absorbing at 470 nm appears. From quenching experiments using LiI, the latter can be attributed to the radical cation $Mc2^+$. The rate constant of back electron transfer k_b (eq 2) is typically of the order of 10^7 s^{-1} and differs very little between adsorbed monomers and aggregates.

Immersed in water at pH = 2.5 the dye-coated TiO_2 film shows a mixture of adsorbed species. Monomers coexist with H- and J-aggregates. Even though the J-aggregate peak at 620 nm hardly absorbs at the excitation wavelength of 532 nm, an important bleaching of the latter is observed upon laser excitation of coexisting monomers and H-aggregates on the substrate surface using the doubled Nd:YAG line (Figure 7). The transient bleaching shows one red-shifted band which is quite broad for a J-aggregate. Also the H-aggregate bleaching can be observed, but the transient absorption of the monomer is absent. Two different mechanisms can be invoked to rationalize this finding (abbreviations M and J will be used to designate the monomer and J-aggregate, respectively):

(i) energy transfer reaction from monomers to the J-aggregates:

$$M^* + J \rightarrow M + J^* \quad (3)$$

$$J^* \rightarrow J^+ + e_{cb}^-(TiO_2) \xrightarrow{k_b} J \quad (4)$$

(ii) electron transfer reaction from J-aggregates to monomers:

$$M^* \rightarrow M^+ + e_{cb}^-(TiO_2) \quad (5)$$

$$M^+ + J \rightarrow M + J^+ \quad (6)$$

Equation 4 can easily be verified by exciting the J-aggregate band at 614 nm using a ruby pumped dye laser. The transient spectrum obtained shows an important bleaching of the J-aggregate concomitantly to the positive absorption change of the oxidized species at 470 nm, which confirms that these red-shifted aggregates are able to inject into TiO_2. A less important bleaching of the H-aggregate appears at 500 nm. Its absorption tail reaches into the red spectral domain, and a small fraction of H-aggregates are also excited by the 614 nm line.

Since J-aggregates are known to be highly emissive, a characteristic fluorescent band is expected if the energy transfer reaction took place (eq 3). The emission of dye-coated TiO_2 films in water is very weak. Nevertheless a weak and broad band with maximum at 630 nm can be observed when exciting at 500 nm, a wavelength where the J-band absorption is vanishing. No evidence was found for reaction 6 using nanosecond laser flash photolysis. Enhanced time resolution might reveal if electron transfer from J-aggregates to monomers takes place.

For important dye loading and when the TiO_2 film is left in a humid atmosphere for 2 days, a double-banded absorption spectrum shows up (see Figure 6). The transient spectrum shows the bleaching of two bands together with the oxidized species at 470 nm (Figure 8). The feature at 550 nm cannot be attributed to the bleaching of the monomer since it is red shifted

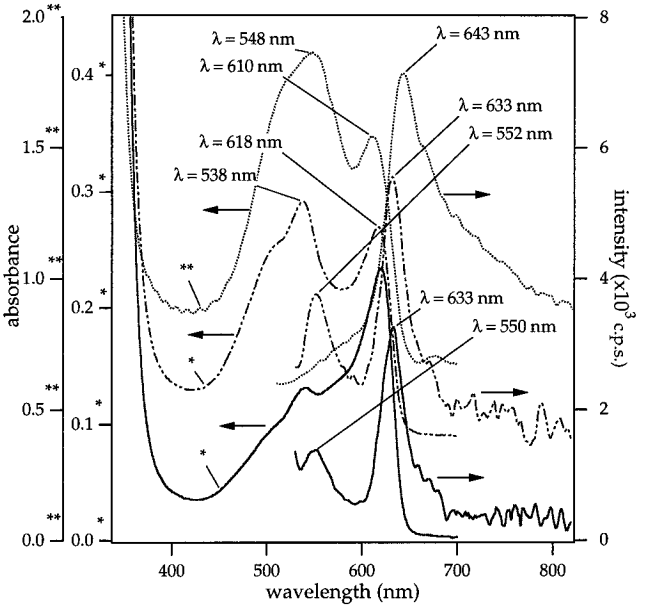

Figure 6. Absorbance and emission spectra of Mc2 adsorbed on a mesoscopic TiO_2 film at room temperature in contact with water vapor at a relative humidity of 50% (—••—) and at a relative humidity of 100% (—). In one case (•••), the dye loading is more important and the sample was exposed to humid air for 2 days. In all three cases, the excitation wavelength is 490 nm.

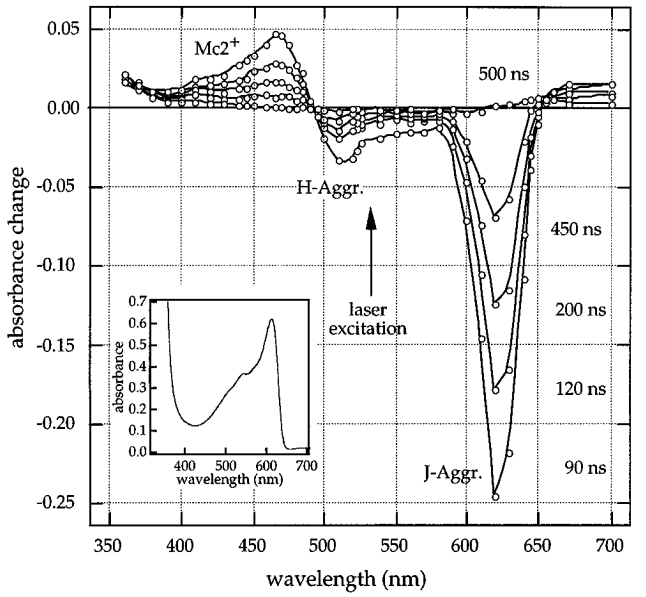

Figure 7. Transcient absorption spectrum obtained upon laser flash photolysis at 532 nm of an Mc2-loaded mesoscopic TiO_2 film in water at pH = 2.5. The inset shows the absorption spectrum. Times after the laser pulse at which the spectra were taken are marked in the graph.

too much and also because no monomer fluorescence is observed. The above facts lead us to the conclusion that the double-banded absorption feature is due to a single aggregate type with two allowed optical transitions. Further evidence for this finding will be given below.

Aggregation of Mc2 Loaded on Salt-Impregnated Mesoscopic Metal Oxide Films. (a) Substrate Treatment. Up to now we have been studying the aggregation of Mc2 on different hydroxylated metal oxide substrates. In this section we present another way of producing aggregates. Instead of using the surface properties of the metal oxide, we take advantage of the porous network built by interconnected particles. The fact that Mc2 is not soluble in highly ionic aqueous salt solutions is used to induce aggregation.

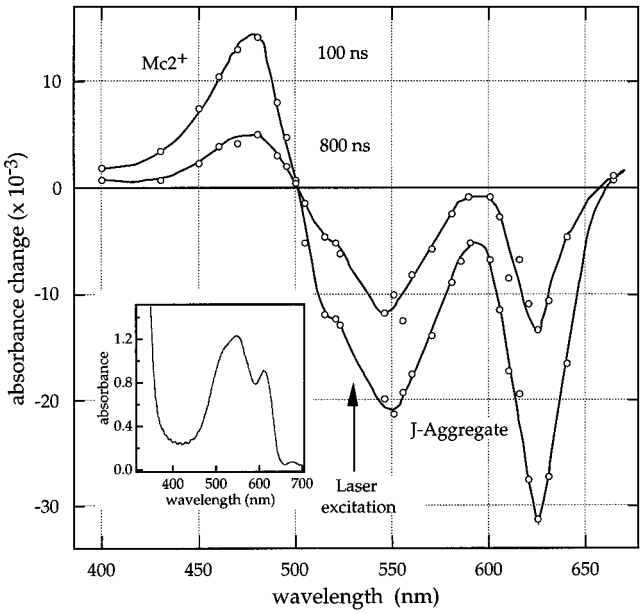

Figure 8. Transient absorption spectrum obtained upon laser flash photolysis at 532 nm of an Mc2-loaded mesoscopic TiO_2 film in nitrogen of 50% relative humidity. Times after the laser pulse at which the spectra were taken are marked in the graph.

We proceed as follows. First the mesoscopic films are loaded with merocyanine dye by dipping in a saturated Mc2 solution in ethanol. After drying, a droplet of 0.8 M aqueous NaOH is spread onto the film by the help of a microscope slide. After complete dispersion of the liquid droplet, the slide is removed. Immediately the color changes to pale yellow. While the dye-coated film is allowed to dry, a very pronounced color change occurs from pale yellow to dark blue. If further drying is allowed, the color turns red again. Apparently the water content of the salt-impregnated mesoscopic film is determining the spectral change. In order to control the relative humidity, a thermostatic cell is used. The sample compartment contains the dye film in contact with the vapor over a saturated aqueous salt solution in equilibrium with an excess of salt. By this means the relative humidity can be adjusted by varying the temperature. In the present case we used a saturated KBr solution to control the humidity. Raising the temperature from 20 to 25 °C leads to a change in the partial water pressure from 19 to 26 mbar.[57] Indeed varying the temperature in the above range leads to a spectral change of the dye-loaded and NaOH-impregnated porous film. The spectral change is not due to a temperature effect, since it can also be produced by changing the partial water pressure at constant temperature using different saturated salt solutions.

(b) The Effect of Water. A dye-loaded and salt-impregnated Al_2O_3 film in a dry atmosphere shows the monomer and H-aggregate band. The same is true for ZrO_2 and TiO_2 films. In particular no J-aggregate band appears even on TiO_2 due to the hydroxide salt surface coating. As the partial water pressure is raised to about 19 mbar, two red-shifted absorption bands at 541 and 602 nm appear, whereas at higher partial water pressures the blue-shifted H-aggregate absorption feature prevails (Figure 9). The occurrence of a very sharp absorption band, like the one at 602 nm, is well-known for J-aggregates and indicates a perfect coherence between the stacked molecules.

Since only one isosbestic point is apparent in Figure 9, the two red-shifted bands are likely to originate from the same

(57) *CRC Handbook of Chemistry and Physics*, 73rd ed.; Lide, D. R., Ed.; CRC Press, Inc.: Boca Raton, 1992; p 15.

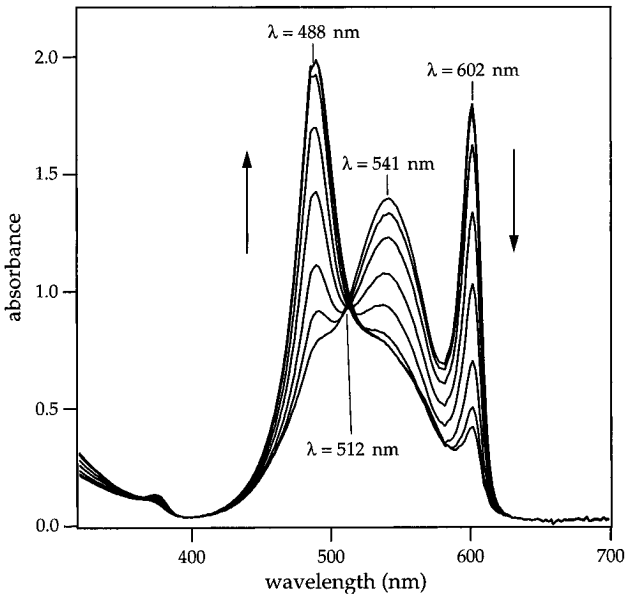

Figure 9. Absorption spectra of Mc2 adsorbed on a transparent Al_2O_3 mesoscopic film impregnated with NaOH. The arrows indicate increasing ambient humidity starting from a partial water pressure (PWP) of about 19 mbar at 20 °C and ending at a PWP of 26 mbar at 25 °C.

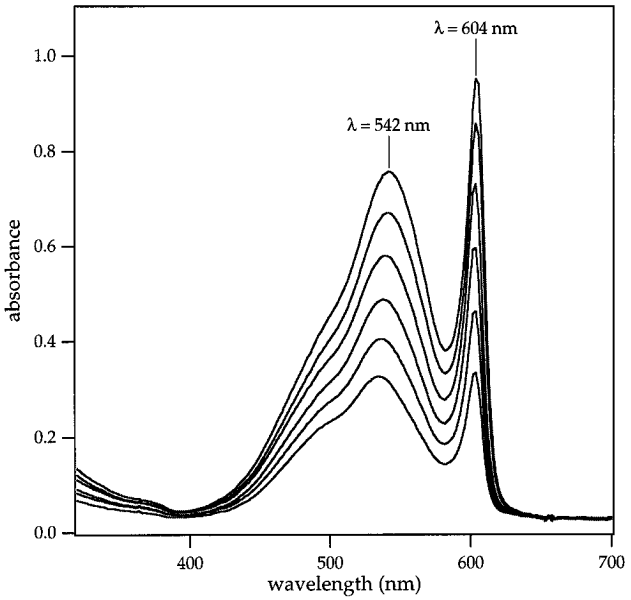

Figure 10. Effect of Mc2 loading on a NaOH-impregnated mesoscopic Al_2O_3 film at a partial water pressure of about 19 mbar at 20 °C. Each step corresponds to a 5 s dipping in an Mc2-saturated ethanol−toluene (1:10, v/v) mixture.

aggregate species. To underline this hypothesis the effect of Mc2 loading is measured at constant relative humidity. For this purpose the mesoscopic Al_2O_3 film is impregnated with NaOH according to the above described procedure. It is then dipped for 5 s in an Mc2-saturated ethanol−toluene (1:10; v/v) mixture and dried at room temperature. Then the film is put into the cell and the absorption spectrum recorded. This process was repeated several times in order to raise the Mc2 loading of the film. Using a nonpolar liquid to adsorb the dye prevents dissolution of the NaOH salt necessary to form J-aggregates. The result displayed in Figure 10 shows a linear increase of the spectral feature, in accordance with the hypothesis of a single species giving rise to the two absorption bands. If an equilibrium between two different species existed, a concentration

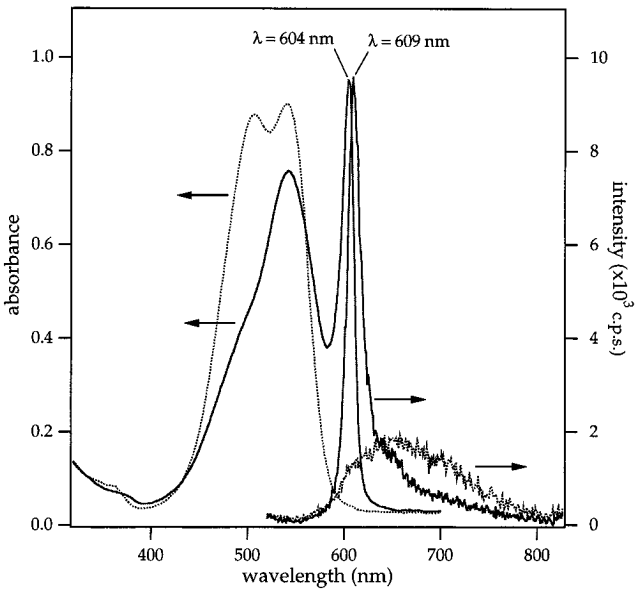

Figure 11. Absorption and emission spectra of Mc2 loaded on a NaOH-impregnated mesoscopic Al_2O_3 film under dry conditions (···) and at a partial water pressure of 19 mbar (—). The excitation wavelength is 490 nm.

dependence would be expected. The same observations are made on porous ZrO_2 films.

The fluorescence spectra of Mc2 on NaOH-impregnated Al_2O_3 films under humid conditions (partial pressure of about 20 mbar) clearly show the resonance feature expected for highly ordered J-aggregates (Figure 11). Furthermore no other emission features are seen in the spectrum. Since the excitation was chosen at 490 nm, a wavelength where the absorption of the narrow band at 604 nm is vanishing, internal conversion from the energetically higher lying band to the lower must take place. The excitation spectrum recorded at an emission wavelength of 611 nm has an important contribution from the absorption band at 541 nm underlining the latter finding. In a dry atmosphere the emission is weaker and very broad. The excitation spectrum shows that it can be attributed to the H-aggregate.

On salt-coated ZrO_2 at a partial water pressure of about 20 mbar, the same luminescence behavior can be observed as for the Al_2O_3 substrate. Again efficient internal conversion takes place from the energetically higher lying exciton band to the lower. At liquid nitrogen temperature a broad band appears, which is similar to the emission of a sample under dry atmospheric conditions at room temperature. We ascribe this observation to a change in the relative humidity during the cooling process. Water condensation at the cryostat sample compartment walls takes place, and the J-aggregate is destabilized.

A similar behavior is found for salt-impregnated TiO_2 films. Again a double-banded red-shifted or a single-banded blue-shifted spectrum is obtained depending on the partial water pressure of the ambient in contact with the film. The aggregation behavior on hydroxylated TiO_2 substrates (not salt impregnated), described in the previous section, can no longer be observed.

(c) Crystal Packing and Reflectance of Mc2 Sodium Salt Single Crystals. Millimeter-long needles of the merocyanine sodium salt octahydrate (MSOH) can be grown from alkaline solutions.[53] There is a striking resemblance between the features of the reflectance spectrum and those of the absorption spectrum of Mc2 aggregates on salt-coated metal oxide films in a humid atmosphere. Again a broad band at 535 nm and a sharp one at

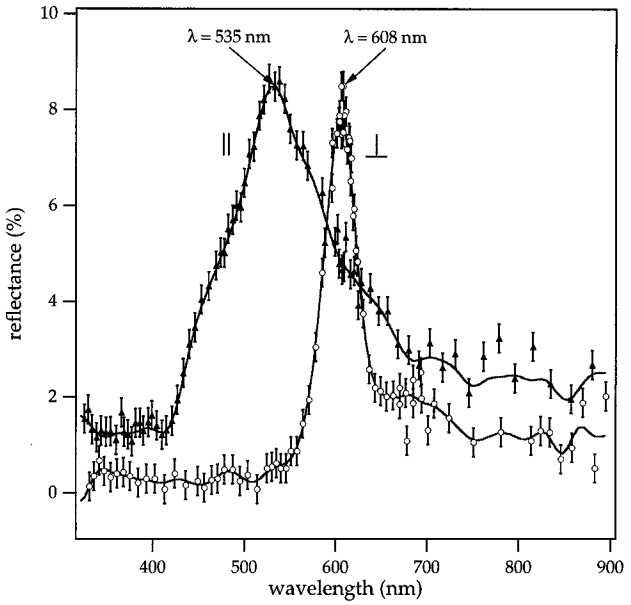

Figure 12. Reflectance spectrum of the Mc2 sodium salt octahydrate single crystal. The polarization parallel (∥) and perpendicular (⊥) to the needle axis of the crystal is indicated in the graph. The directions parallel and perpendicular correspond to the *c* and *d* axes of Figure 13, respectively.

608 nm can be seen (Figure 12). Furthermore the two bands are polarized orthogonal to each other, parallel and perpendicular to the needle axis of the crystal. These directions correspond to the *c* and *d* axes in Figure 13, respectively.

Small Mc2 sodium salt microcrystals can easily be obtained by slow precipitation of Mc2 in saturated water solution using sodium hydroxide. The Kubelka−Munk remission function[58] of sodium salt microcrystals diluted in BaF_2 powder shows two absorption bands that correspond exactly to the spectral feature of Mc2 on mesoporous, salt-impregnated metal oxide films under humid conditions. A similar diffuse reflectance spectrum is obtained using Mc2 calcium, strontium, and barium salt microcrystals precipitated from an aqueous solution using the respective hydroxide salts. They suggest a similar packing of the merocyanine molecules.

Of valuable help in linking the J-aggregate spectrum to its geometry is the recently determined single-crystal structure of MSOH.[53] This structure consists of a layered architecture with alternating 14.5 Å thick organic layers containing the Mc2 anions and 7.2 Å thick inorganic layers containing the water-coordinated sodium cations. The cross section parallel to the organic layer plane shows a two-dimensional herringbone structure arrangement of Mc2 molecules (Figure 13). The center to center distance between two translationally equivalent molecules is 7.01 Å, and a slipping angle betwern two nearest neighbors of 29.9° can be defined, which is typical for J-aggregates. Furthermore, the molecules are oriented edge-on with respect to the aqueous sodium cation planes with the carboxyl and carbonyl groups pointing toward the inorganic phase, a geometry which has already been proposed for the orientation of cyanine molecules adsorbed on silver halide single crystals.[7,23] The molecular plane of the dye molecules is not exactly perpendicular to the inorganic layer but builds a dihedral angle of 74.1° with the latter, which seems to be due to the steric repulsion of the acetyl and ethyl groups.[53] Interestingly the metal cations are not building a chelate with the carboxyl and carbonyl groups as proposed for the formation of J-aggregates using the LB technique.[59] Figure 14 shows that the Na^+ cations are octahedrally coordinated by water molecules and only indirectly linked to the organic anions by Coulombic interaction and hydrogen bonding between the cation's solvation shell and the dye's carbonyl and carboxyl group, respectively. Also seen in the picture are water molecules within the organic layer, linked by hydrogen bonds.

(d) Counterion Effect. The split J-absorption peak observed for NaOH-impregnated mesoscopic films also appears by coating the metal oxide substrates with a 0.8 M aqueous KOH or RbOH solution. However, when a stoichiometric amount of 18-crown-6 ether is added to the NaOH or KOH solutions, no J-aggregate feature can be observed.

Salt impregnation by LiOH or ammonium hydroxides does not produce J-aggregates, nor did the substrate coated with alkali chloride salts in equal concentrations show the new J-aggregate feature in humid air.

These results suggest that a hygroscopic hydroxide salt is needed for the formation of J-aggregates in humid air. Furthermore, the cation has to be small enough to assist the geometrical construction of the molecular assembly which gives rise to the J-aggregate bands. The Li^+ cation seems to play a special role. The proton-like character of the latter might be responsible for the absence of J-aggregate formation. Mc2 lithium salt solvate single crystals can be grown from alkaline solutions similarly to the MSOH crystals. Figure 15 shows a projection of the Mc2 lithium salt crystal structure.[53] The distorted tetrahedral oxygen surrounding of the Li^+ cations consists of two oxygen atoms coming from the carboxyl functional groups of two Mc2 molecules and two oxygen atoms coming from solvent molecules. Thereby the closest Li−O distance of 1.91 Å is formed between the Li^+ cation and a carboxyl oxygen of the Mc2 anion.

Discussion

Until now no stable J-aggregate solutions of the unsymmetrical merocyanines have been reported , except for dispersions of microcrystallites in water solutions.[60] In the case of the LB technique, J-aggregates are formed at the subphase−air interface using long alkyl substituents. It has also been proposed that long alkyl chains would be necessary for aggregate stability. Our method uses mesoporous substrates and allows the formation of J- as well as H-aggregates of a merocyanine dye having no long alkyl substituents. Two approaches have been presented in the Results section. The first uses hydroxylated metal oxide films, whereas the second requires impregnation of the porous films with a hydroxide salt.

Let us first discuss aggregation in salt-impregnated mesoporous films. In humid air the hygroscopic salt precipitated in the pores is dissolved by taking up water. As the partial water pressure is raised, an aqueous film will be built on the substrate surface, thereby producing an air−water interface. If more water is taken up, the pores will be completely filled by the aqueous hydroxide salt solution. This mechanism is also valid for other hygroscopic salts. Alkali chloride salts, however, do not show the aggregation effect.

Hydroxide groups are needed to negatively charge the substrate surface, thus preventing the dye to adsorb onto the metal oxide surface. Since the dye is not soluble at high ionic strength, it will either assemble at the air−water interface or precipitate within the pores if no such interface is present. Therefore, the aggregate size will be determined by the pore size, and if the pore size distribution is uniform, the same is

(58) Kortüm, G. *Reflectance Spectroscopy*; Springer: Berlin, 1969.

(59) Kawaguchi, T.; Iwata, K. *Thin Solid Films* **1989**, *180*, 235.

(60) Kasai, H.; Nalwa, H. S.; Oikawa, H.; Okada, S.; Matsuda, H.; Minami, N.; Kakuta, A.; Ono, K.; Mukoh, A.; Nakanishi, H. *Jpn. J. Appl. Phys.* **1992**, *31*, L1132.

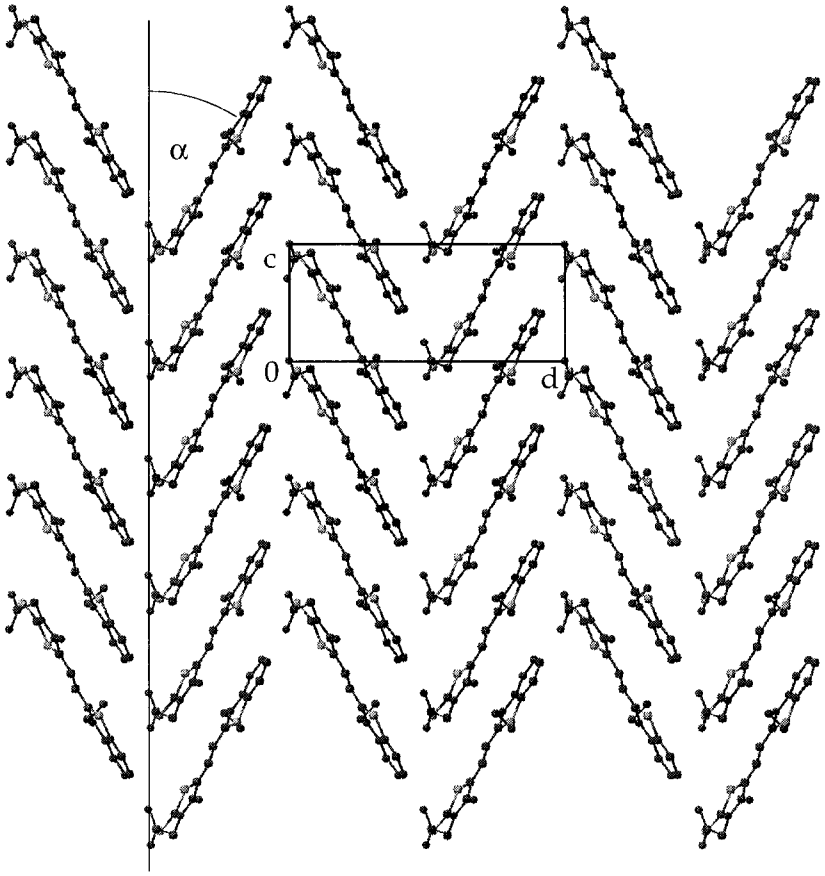

Figure 13. Cross section of the Mc2 sodium salt octahydrate single-crystal structure showing a top view of the organic layers. Hydrogen atoms and water molecules are omitted for clarity. The two-dimensional unit cell parameters are $d = 16.583$ Å and $c = 7.005$ Å. The slipping angle is $\alpha = 29.9°$.

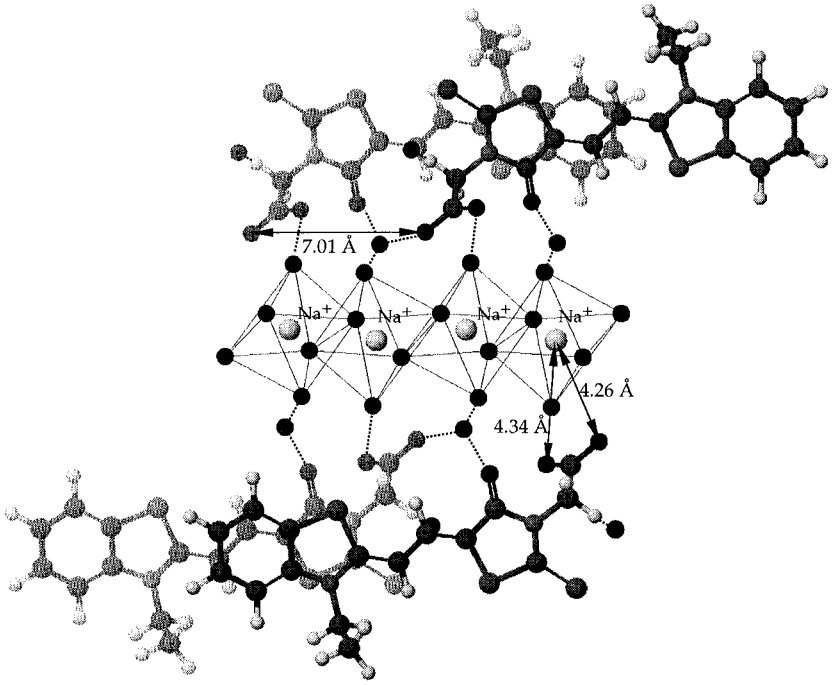

Figure 14. Section of the Mc2 sodium salt octahydrate single-crystal structure showing the octahedrally coordinated Na^+ cations that are coupled to the carboxyl functional group of Mc2. Hydrogen atoms belonging to water oxygens are omitted for clarity. Hydrogen bonds are indicated by a dotted line, and some characteristic distances are marked in the figure. Water molecules incorporated in the organic layer and linked by hydrogen bonding are also shown.

expected for the aggregate. The narrow absorption bands in Figure 9 show that the size distribution of J- as well as H-aggregates formed in the mesoporous substrates prepared by our method is rather uniform.

When the partial water pressure of the ambient in contact with the dye-loaded film is raised, an isosbestic point is present in the spectrum upon changing from H- to J-aggregates. It suggests that only two species are involved in the optical

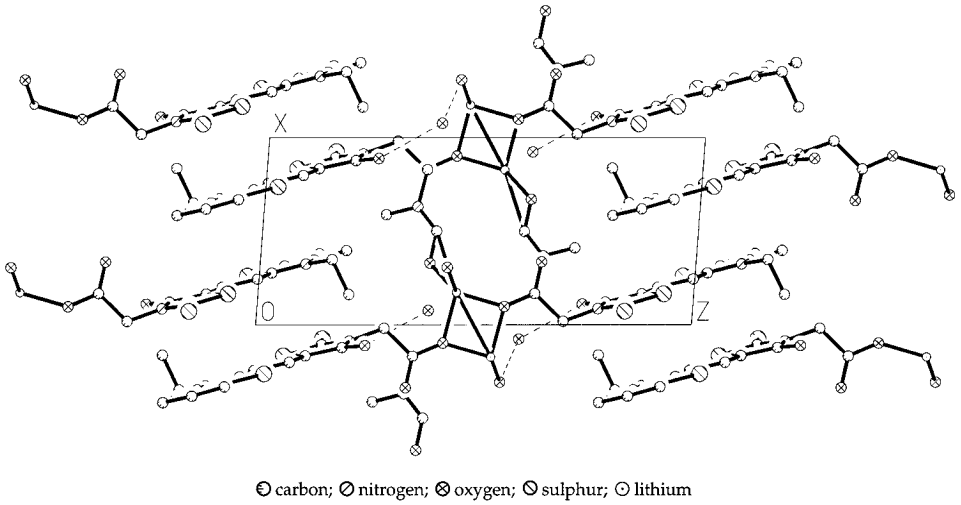

Figure 15. Projection of the Mc2 Li salt crystal structure along the *b* axis.[53] Hydrogen atoms and disordered molecules of dimethylformamide are omitted for clarity. The Li^+ cations have distorted tetrahedral coordination. The two Li···O separations of the O atoms of the acetate group of Mc2 anions are 1.91 and 1.98(1) Å, and the Li···O (dimethylformamide) and Li···O (H_2O) separations are 1.96 and 1.94(1) Å, respectively. The Li···Li separation is 2.77(2) Å.

features. Further evidence is given by measuring the effect of dye loading at constant water vapor pressure. If the split absorption spectrum with maxima at 541 and 604 nm were due to the equilibrium between two different aggregate species, a concentration dependence of the relative heights of the absorption maxima would be expected. However, the feature of the double-banded spectrum does not vary when the dye loading is increased on the same substrate. Luminescence, too, underlines the hypotheses of a single species giving rise to the two absorption maxima. Excitation at 490 nm, a wavelength where light absorption arises from the broad band centered at 541 nm, shows fluorescence only from the narrow band at 604 nm. This indicates that internal conversion from the energetically higher lying band of the aggregate to the lower takes place. The close resemblance between the spectrum of Mc2 on salt-impregnated metal oxide surfaces and the one of sodium salt single crystals suggests a similar type of molecular packing. This analogy is further supported by the interfacial architecture of the crystal.

The Mc2 anions in the sodium salt single crystals are packed in a two-dimensional herringbone type structure with two translationally inequivalent molecules per unit cell. According to exciton theory, the number of exciton bands corresponds to the number of translationally inequivalent molecules per unit cell.[28] Indeed, the single-crystal reflectance spectrum shows two bands separated by an important Davidov splitting of 0.28 eV. Similarly to another work,[8] the two transitions are perpendicularly polarized. This can well be understood by considering the transition dipole moments of the individual molecules in the two-dimensional organic plane. These dipole moments are oriented almost parallel to the molecular axis.[52] Two dipole arrangements are predicted to yield important transition probabilities.[61] The out of phase arrangement (sum of the dipole moments perpendicular to the *c* axis of Figure 13) results in lowering the energy and gives rise to the band at longer wave lengths. The in-phase arrangement (sum of the dipole moments parallel to the *c* axis) raises the transition energy and corresponds to the band at shorter wave lengths. The difference in width between the two exciton bands has already been observed in the past[62] and was proposed to be due to phonon coupling.[63]

In order to rationalize the counterion effect on the two-dimensional J-aggregates, the Mc2 sodium salt octahydrate (MSOH) crystal structure provides a helpful model. Due to the layered structure in the case of the MSOH consisting of a 7.2 Å thick aqueous phase alternating with a 14.5 Å thick organic phase, interactions between the organic and inorganic layers in the crystal can be compared to the interactions at an ionic aqueous interface.

In the MSOH structure, each sodium cation is coupled to the anionic carboxyl functional group of the dye by Coulombic interaction (Figure 14). In a similar way J-aggregation at the air−water interface might be assisted by the solvated cations of the aqueous phase. When the cation is too bulky, e.g., when it is bound to a crown ether, the merocyanine anions which are coupled to the bulky cations can no longer approach each other to the distance necessary for the J-aggregate formation. As a consequence the absorption spectrum shows only the presence of H-aggregates and monomers. In the case of Li^+ cations, J-aggregation is absent as well. The proton like character of the small cation seems to be responsible for this observation. As is suggested by the Mc2 Li salt solvate crystal structure, the partial solvation of Li^+ allows the cation to come much closer (≈1.9 Å) to the carboxylic group of Mc2 than the solvated sodium cation (≈4.2 Å). In this way the formation of the two-dimensional herringbone structure is inhibited.

The spectral change upon raising and lowering the humidity is reversible up to a few cycles but can no longer be observed after a few days. The major factor causing irreversible degradation is the nucleophilic attack of hydroxide anions on an sp^2 carbon atom, yielding first a yellow highly fluorescent species, which is subsequently degraded to a colorless product. According to semiempirical calculations (ZINDO-CI) the carbon atom of the carbonyl functional group seems to be the most likely to undergo nucleophilic attack. This process is thermally activated and can well be observed in alkaline solutions, too.

While salt-impregnated films behave almost the same for Al_2O_3, ZrO_2, and TiO_2, important differences in the aggregation behavior are observed between the three oxides when the substrates are not salt impregnated. It is striking that surface-induced J-aggregation could only be observed on hydroxylated and protonated TiO_2 colloidal substrates and is absent on hydroxylated, protonated colloidal Al_2O_3 and ZrO_2 surfaces even though strong physisorption occurs. Even more conspicuous

(61) Czikkely, V.; Försterling, H. D.; Kuhn, H. *Chem,. Phys. Lett.* **1970**, *6*, 11.

(62) Hong, H.-K.; Robinson, G. W. *J. Chem. Phys.* **1971**, *54*, 1369.

(63) *Excited States*; Lim, E. C., Ed.; Academic Press: New York, 1974; Vol. 1, p 101.

is the observation that TiO_2 substrates prepared by different methods but with the same surface treatment do not always induce J-aggregation.

As a first explanation, epitaxial adsorption may be invoked, which is assumed to play a role in the formation of cyanine J-aggregates on silver halides.[6,7] In the case of Mc2, specific surface interaction with the carboxyl and carbonyl groups of the dye orients the latter edge-on with respect to the metal oxide surface. On hydroxylated, protonated surfaces, this kind of binding is likely to be of the same type as on highly ionic aqueous surfaces; i.e., it involves the Coulombic interaction between the carboxylic group and the positively charged surface sites as well as hydrogen bonding to water molecules.

For epitaxial adsorption to be relevant, the geometry of positively charged surface anchor groups has to correspond to a particular aggregate periodicity. As seen in Figure 13, a center to center distance of 7.01 Å and an interplanar distance of 3.4 Å between neighboring molecules are characteristic for Mc2 J-aggregates. The porous TiO_2 films used in this work consist of anatase particles exposing preferentially the (101) crystal face as was determined by HRTEM (Figure 1). The preferential orientaiton of (001) and (101) surface planes has already been reported for natural and synthetic anatase single crystals.[64] The same observation has been reported for P25 anatase particles 22 nm in diameter.[65] However, none of the two planes gives a satisfying epitaxial fit between the surface lattice sites and the J-aggregate geometry of Figure 13.

Contrary to the J-aggregation on salt-impregnated films, J-aggregation on hydroxylated TiO_2 films results in a variety of different red-shifted absorption bands depending on the vapor composition of the ambient in contact with the film. In humid air two kinds of J-aggregates are observed. They differ not only in the absorption peak position but also by their luminescence. One absorption band is located at 620 nm and is due to a single J-aggregate for which exciton theory predicts parallel alignment of the molecules. This aggregate is in equilibrium with another species located around 540 nm that can be identified from the fluorescence spectrum. The absorption and fluorescence maxima coincide with the ones of monomeric Mc2 in water. It is, however, not excluded that an aggregate could yield a similar spectroscopic feature. The other spectrum consists of a split absorption band and is the signature of one aggregate species. Similarly to the herringbone J-aggregates on salt-impregnated films, internal conversion leads luminescence to occur only from the energetically lower lying band. The occurrence of both single- and double-banded J-aggregates on TiO_2 is underlined by the fact that both species do inject into TiO_2 and therefore can be identified by their transient absorption spectra.

The above observations suggest that epitaxy is not the only factor determining the aggregate geometry of the adsorbed dye on hydroxylated, protonated TiO_2 surfaces in water or water vapor. This is not surprising in view of the adsorption model of Figure 14. Coulombic interaction between the carboxyl oxygens of Mc2 and the surface cations is weakened greatly by their large separation as well as by the high dielectric constant of the medium. The strong dependence of aggregate geometry on the atmospheric conditions underlines the relatively weak ionic binding.

In order to explain the absence of J-aggregates on ZrO_2 and Al_2O_3 the surface morphology of the mesoscopic particles can be invoked. Figure 1 depicts HRTEM micrographs of the sintered particles that were scratched off the films. TiO_2 colloids that form the porous films show cubic to rhombohedral shapes and present terraces with an approximate dimension of 10−15 nm in diameter. Such planes are not seen for ZrO_2 and Al_2O_3. In the latter case most of the atomically flat surfaces have a dimension of a few nanometers only and are not likely to provide terraces large enough for the formation of two-dimensional J-aggregates. Therefore the surface morphology might strongly influence aggregation. The two-dimensional nature of J-aggregates suggests that an atomically flat surface is needed, large enough to accommodate the number of molecules necessary for their aggregate stability. The lack of such planes as in the case of the spherically shaped ZrO_2 and highly rough Al_2O_3 particles is in agreement with the absence of any J-aggregate band.

Commercial powders can be used to corroborate this finding. P25 (Degussa) powder consists of a mixture of rutile and anatase TiO_2 particles. Recent studies on the morphological modification of heated microcrystalline P25 particles have revealed that the original small plate-like particles are transformed into larger round particles after firing at 1100 °C. Smaller crystallites protrude on the particle surface.[66] Adsorption of Mc2 on P25 shows that J-aggregation is only obtained on the unfired powder and is inhibited by firing.

The absorption and emission bands of J-aggregates on TiO_2 are quite broad compared to the ones on salt-impregnated films exposed to humid air. As a result no resonance fluorescence is observed which gives rise to a Stokes shift of about 0.05 eV. The width of the J-aggregate band can be explained by the nonhomogeneous size distribution of the two-dimensional aggregates. In fact the size distribution of atomically flat surface planes of the sintered TiO_2 particles will give rise to aggregates of different dimensions.

In summary, we have demonstrated an easy method to induce J- and H-aggregation of carboxylated merocyanine dyes by impregnating highly porous metal oxide substrates with a hydroxide salt. When the atmospheric partial pressure of water is raised, more and more water is taken up by the salt, building an aqueous film on the substrate surface. Furthermore, the metal oxide surface is negatively charged by hydroxide ions and the dye is desorbed and assembles at the air−water interface to form J-aggregates in a herringbone structure (Figure 16a). If the partial water pressure is raised beyond 20 mbar, there is no possibility for the Mc2 molecules to build two-dimensional assemblies at an air−water interface and yellow H-aggregates showing a columnar stacking geometry are formed within the pores (Figure 16b). If the porous films are not salt impregnated, two-dimensional J-aggregates can only be built on monoatomically flat surface planes that are large enough to accommodate the aggregate. A variety of different J-aggregate structures can be induced by varying the solvent vapor pressure in the ambient that is in contact with the hydroxylated and protonated film, suggesting that surface epitaxy is not important.

Conclusions

Hydroxylated and salt-impregnated films have been used to scrutinize H- and J-aggregation of a merocyanine dye. A new method has been developed to form and spectroscopically analyze aggregates on mesoporous oxide substrates under distinct atmospheric conditions. The high porosity of the transparent colloidal films enlarges the dye-coated interface and facilitates by this means the spectroscopic analysis. Similarly to the Langmuir−Blodgett technique the hydrophobic force is

(64) Hartman, P. In *Crystal Growth*; Hartman, P., Ed.; North-Holland: Amsterdam, 1973; p 367.

(65) Munera, G.; Moreno, F.; Gonzalez, F. In *Reactivity of solids*; Anderson, J. S., Roberts, M. W., Stone, T. S., Eds.; Chapman and Hall: London, 1972; p 681.

(66) Cerrato, G.; Marchese, L.; Morterra, C. *Appl. Surf. Sci*. **1993**, *70/71*, 200.

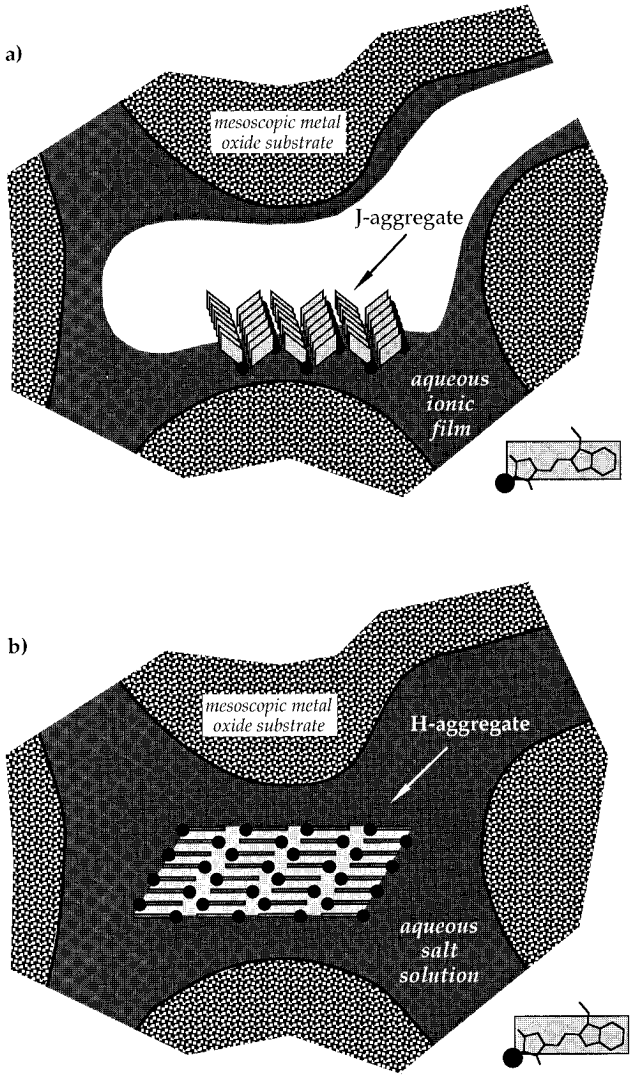

Figure 16. Effect of water uptake by porous metal oxide films impregnated with a hydroxide salt. The merocyanine dye is represented by a gray rectangle, and the carboxyl functional group is indicated by a black point: (a) film in contact with an ambient of 50% relative humidity; (b) film in contact with an ambient of 100% relative humidity.

used to assemble the dye at the salt solution surface. At the very high ionic force used in this approach there is no need for long alkyl chains since Mc2 is not soluble at such salt concentrations. Our study also shows that long alkyl substituents are not needed to stabilize J-aggregates as has been proposed by different authors.

The previously determined layered organic−inorganic crystal structure of the Mc2 sodium octahydrate[53] allows one to rationalize the observed split absorption spectrum in terms of a herringbone type structure with an adsorption edge-on with respect to the surface of the salt-impregnated oxide films under humid conditions. Water uptake of the salt leads to the formation of a highly ionic aqueous phase within the mesoporous network. The polar group (carboxylic group) of Mc2 points toward the salt solution and pairs with a hydrated metal cation. Thereby the dye molecules are oriented, which assists the formation of the appropriate aggregate geometry. Intercalated solvent molecules stabilize the structure. We successfully applied this method to build herringbone-structured J-aggregates within the mesoscopic pore structure of ZrO_2, Al_2O_3, and TiO_2 films. The aggregate size on salt-impregnated films is determined by the size of the micropores and is not influenced by the surface properties of the bare substrate. Resonance fluorescence from the J-band indicates that coherence within the aggregate is excellent.

On TiO_2 particles of 20−30 nm the hydroxylated, protonated surface attracts the dye, orienting it edge-on with respect to the positively charged surface. The carboxyl and carbonyl groups are not likely to chelate the hydroxylated and protonated titanium surface atoms, but are linked by Coulombic interaction and hydrogen bonding to the charged surface. Due to the high dielectric constant of the medium, the electrostatic interaction is strongly reduced and intermolecular van der Waals forces become important. This explains the ease with which changes in the aggregation geometry can be induced just by varying the partial solvent vapor pressure in the ambient contacting the film. As discussed above, solvent molecules are intercalated between the organic dye molecules and stabilize either one or the other geometry depending on the vapor pressure. Two J-aggregate structures could be obtained, one showing a split absorption spectrum, the other showing a single absorption band. Epitaxial growth of the herringbone structure can be ruled out by the fact that the predominant anatase surface planes (i.e., the (001) and (101) planes) do not match the aggregate lattice geometry in the crystalline form.

Neither untreated sintered Al_2O_3 colloidal films nor ZrO_2 films show red-shifted spectra when Mc2 is adsorbed on the hydroxylated and protonated surface (this surface has to be distinguished from the salt-impregnated surface mentioned above). Even more decisive, J-aggregates are formed on platelike P25 (Degussa) anatase particles but are inhibited when adsorbed on fired P25 particles with a highly disordered surface. This fact underlines that the surface morphology is crucial for the growth of aggregates. Terraces large enough to accommodate the number of molecules necessary for the J-aggregate stability are required.

Acknowledgment. We are grateful to Dr. M. Carrard (Laboratoire de physique des solides semi-cristallins, Département de Physique, EPFL, CH-1015 Lausanne, Switzerland) for HRTEM analysis of the Al_2O_3 and ZrO_2 substrates. We are thankful to J. Müller and Dr. L. Degiorgi (Institut für Festkörperphysik, ETHZ, Zürich, Switzerland) for the reflection measurement on single crystals. Financial support of this work from the Swiss National Fund of Scientific Research is gratefully acknowledged.

JA953042+